VOLGA
07.04.22

Колганов Фёдор

The miniJPAS survey: Identification and characterization of the emission line galaxies down to z < 0.35 in the AEGIS field

The Javalambre-Physics of the Accelerating Universe Astrophysical Survey (J-PAS) is expected to map thousands of square degrees of the northern sky with 56 narrowband filters (spectral resolution of $R \sim 60$) in the upcoming years. This resolution allows us to study emission line galaxies (ELGs) with a minimum equivalent width of 10 Å in the Hα emission line for a median signal-to-noise ratio (S/N) of 5. This will make J-PAS a very competitive and unbiased emission line survey compared to spectroscopic or narrowband surveys with fewer filters. The miniJPAS survey covered 1 deg^2 , and it used the same photometric system as J-PAS, but the observations were carried out with the pathfinder J-PAS camera. In this work, we identify and characterize the sample of ELGs from miniJPAS with a redshift lower than 0.35, which is the limit to which the Hα line can be observed with the J-PAS filter system. Using a method based on artificial neural networks, we detect the ELG population and measure the equivalent width and flux of the Hα, Hβ, [O III], and [N II] emission lines. We explore the ionization mechanism using the diagrams [OIII]/Hβ versus [NII]/Hα (BPT) and EW(Hα) versus [NII]/Hα (WHAN). We identify 1787 ELGs (83%) from the parent sample (2154 galaxies) in the AEGIS field. For the galaxies with reliable EW values that can be placed in the WHAN diagram (2000 galaxies in total), we obtained that 72.8 ± 0.4 %, 17.7 ± 0.4 % , and 9.4 ± 0.2 % are star-forming (SF), active galactic nucleus (Seyfert), and quiescent galaxies, respectively. The distribution of EW(Hα) is well correlated with the bimodal color distribution of galaxies. Based on the rest-frame ($u - r$)–stellar mass diagram, 94% of the blue galaxies are SF galaxies, and 97% of the red galaxies are LINERs or passive galaxies. The nebular extinction and star formation rate (SFR) were computed from the Hα and Hβ fluxes. We find that the star formation main sequence is described as $\log \mathrm{SFR}\,[M_\odot \mathrm{yr}^{-1}] = 0.90^{+0.02}_{-0.02} \log M_\star[M_\odot] - 8.85^{+0.19}_{-0.20}$ and has an intrinsic scatter of $0.20^{+0.01}_{-0.01}$. The cosmic evolution of the SFR density (ρ_{SFR}) is derived at three redshift bins: $0 < z \leq 0.15$, $0.15 < z \leq 0.25$, and $0.25 < z \leq 0.35$, which agrees with previous results that were based on measurements of the Hα emission line. However, we find an offset with respect to other estimates that were based on the star formation history obtained from fitting the spectral energy distribution of the stellar continuum. We discuss the origin of this discrepancy, which is probably a combination of several factors: the escape of ionizing photons, the SFR tracers, and dust attenuation, among others.

- Цели:
- Найти галактики с эмиссионными линиями в поле обзора AEGIS
- Определить параметры звёздного населения
- Показать потенциал J-PAS

Sect. 2.3). We selected all the objects detected in miniJPAS with a photometric redshift (photo-z) lower than 0.35, which is the highest redshift at which Hα can be observed in miniJPAS. The

We imposed a maximum class-star probability of 0.1, as defined in `SExtractor`, in order to select only extended sources. We discarded galaxies with an S/N lower than 1.8 in the filters to capture the flux of the emission lines. The estimates of the EWs

The ANNs learned to perform different tasks. First, an ANN was trained to estimate the EW values for the main emission lines in the optical range: Hα, Hβ, [O III], and [N II]. This ANN is re-

fluxes (see MS21 for further details). Second, another ANN was trained to distinguish galaxies with emission lines from those without them. This classifier ($\mathrm{ANN_C}$) also relies on the EWs,

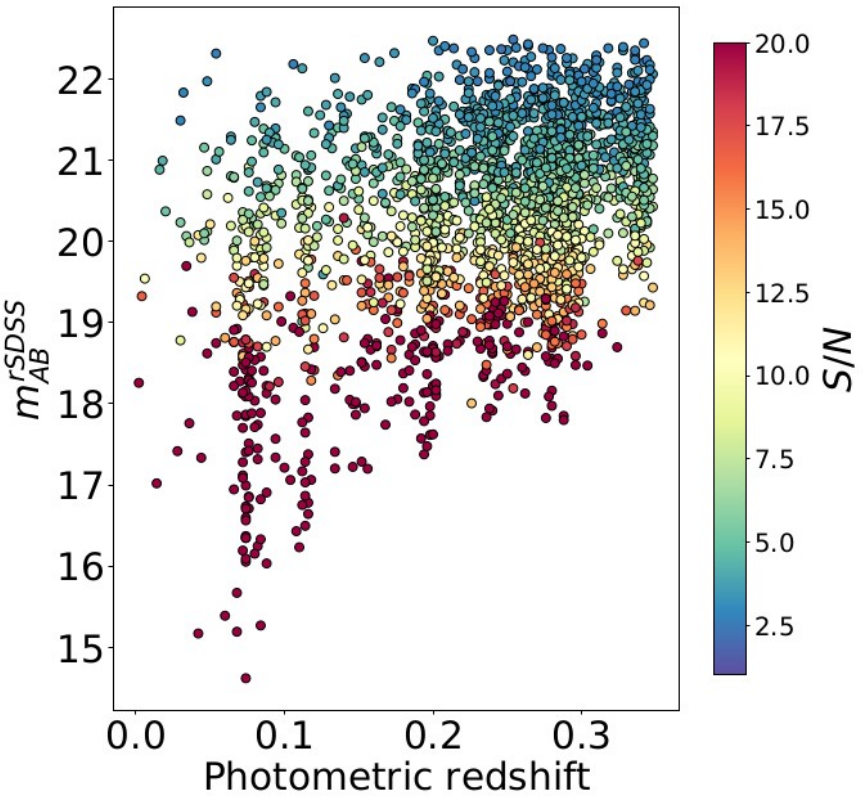

Fig. 1. Relation between the apparent magnitude in the rSDSS band and redshift for all galaxies in the parent sample. We used the `MAG_AUTO` photometry. Dots are color-coded according to the median S/N of the J-PAS narrowband filters.

Stellar population analysis

$$\Psi(t) = \phi \frac{t_0 - t}{\tau} \exp\left[-(t_0 - t)/\tau\right],$$

The code used the 2017 version of the Bruzual & Charlot (2003) stellar population (SSP) synthesis models (hereafter CB17). The SSP covers the metallicity range $\log Z_\star/Z_\odot$ = -2.3, -1.7, -0.7, -0.4, 0, and +0.4, and the ages span from 0 to 14 Gyr. The CB17 models follow the PARSEC evolutionary

It is important to emphasize that filters capturing the nebular emission lines are masked and were not used in the SED fitting. Therefore, the galaxy properties are only based on the stellar continuum, and it does not include the emission of nebular regions or the result of the AGN activity. The stellar continuum

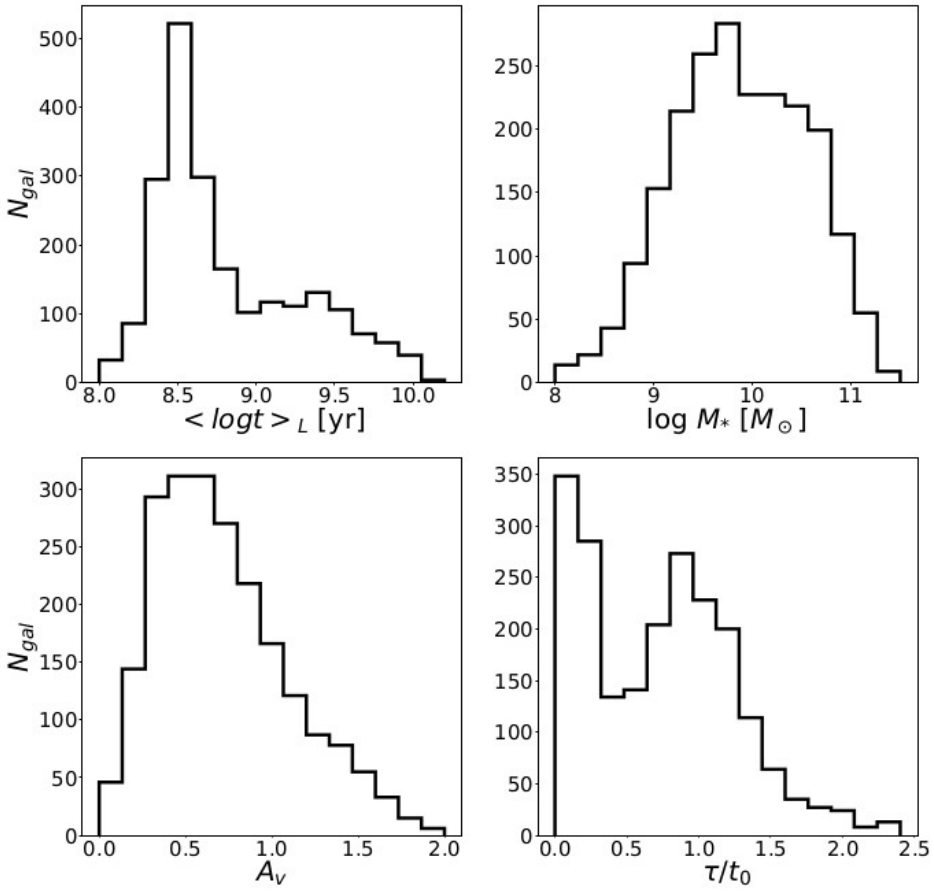

$$(u-r)_{\rm int}^{\rm lim} = 0.16 \times (\log M_\star - 10) - 0.3 \times (z - 0.1) + 1.7. \quad (2)$$

Galaxies with $(u-r)_{\rm int}$ above $(u-r)_{\rm int}^{\rm lim}$ are classified as red galaxies, otherwise, they are considered to be blue. Furthermore,

Generally, blue galaxies are star-forming galaxies, while red galaxies are quiescent. However, a galaxy might appear to be part of the red sequence due to the presence of dust, which absorbs a fraction of the total radiation more efficiently on the blue side of the spectrum. Therefore it is important to correct for dust extinction in order to distinguish between red and dust-reddened star-forming galaxies.

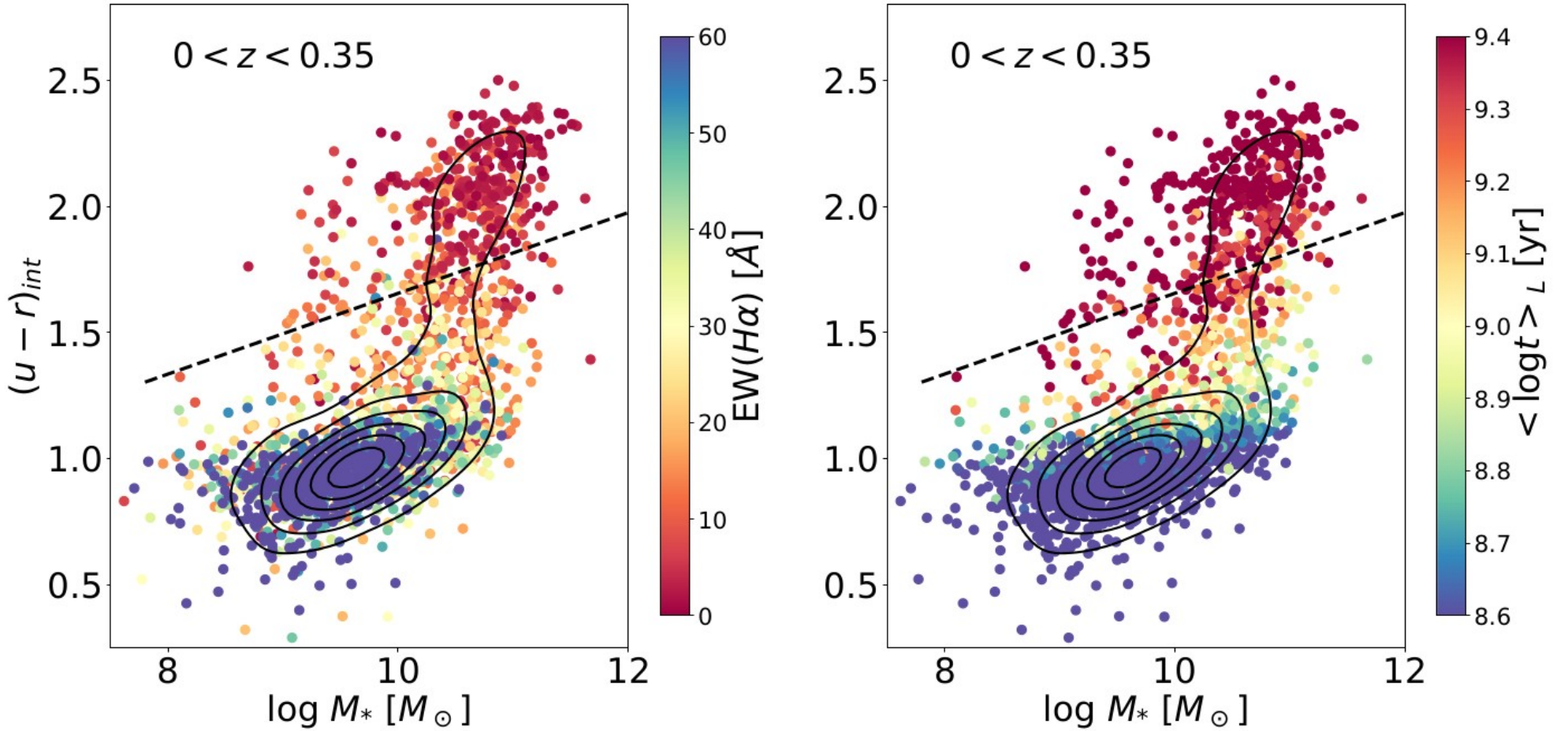

Fig. 5. Color–mass diagram for our sample of galaxies. The (u – r) color-corrected for dust extintion vs. stellar mass. Galaxies are color-coded with the EW of Hα (the luminosity-weighted stellar age) on the left side (right side). The intrinsic color, stellar mass, and luminosity-weighted age are obtained via `BaySeAGal`. Dashed black lines separate blue and red galaxies following Eq. 2, where we considered the median redshift of the sample (z = 0.25). Density contours are drawn in black at the top.

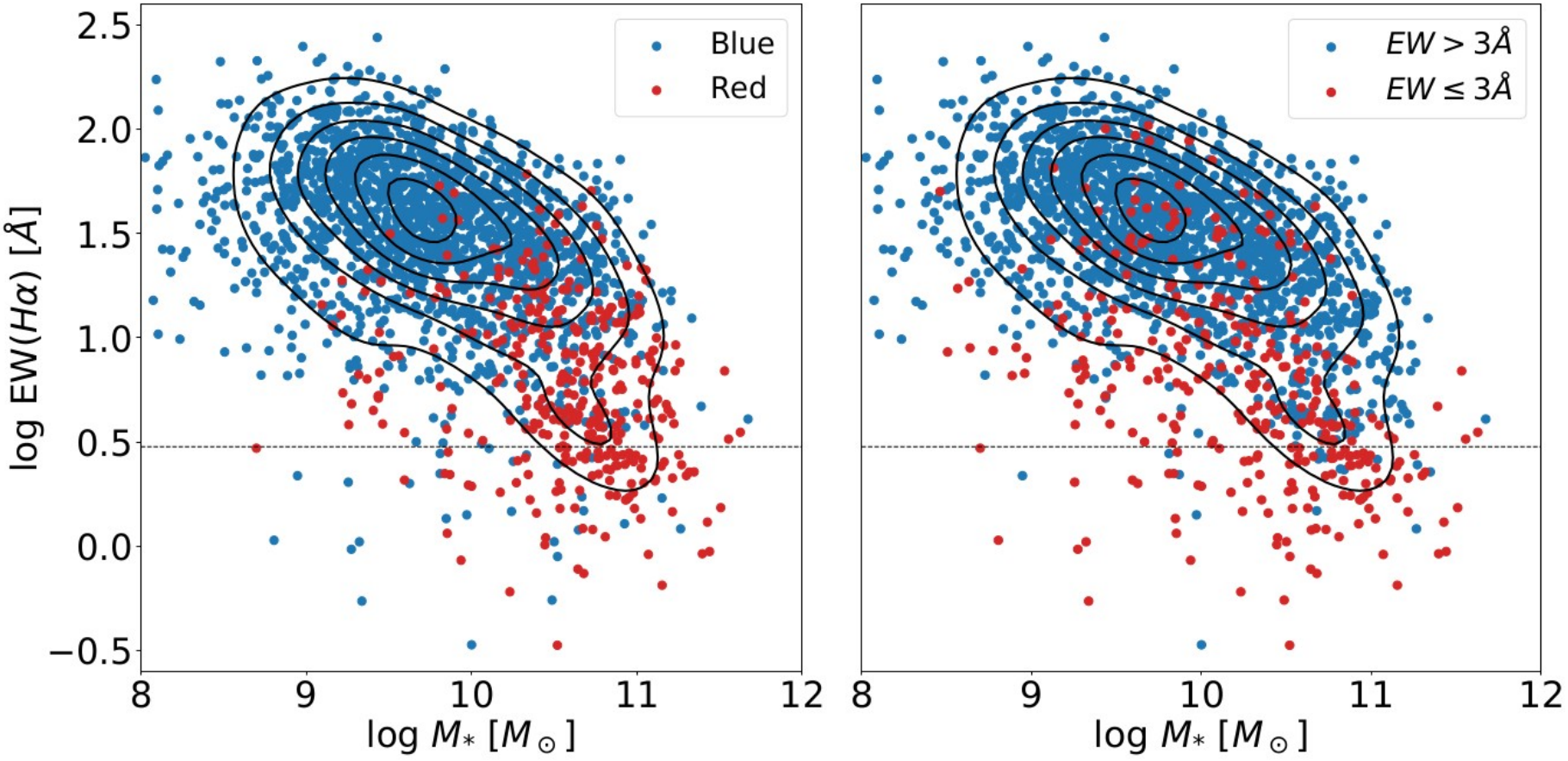

Fig. 6. Equivalent width of Hα as a function of the stellar mass of the galaxy. In the left panel, we used Eq. 2 to distinguish between red and blue galaxies. In the right panel, we relied on the classification performed with a machine-learning code trained with strong EL and weak EL galaxies. Strong ELs were defined as those with EWs greater than 3 Å in any of the following emission lines: Hα, Hβ, [O III], or [N II], and weak ELs are all others. The dashed horizontal lines mark the 3 Å limit in the EW(Hα). Density contours are drawn in black at the top.

Our sample of star-forming galaxies was obtained from the parent sample (Sect. 2) by imposing different constraints. We relied on the WHAN diagram to exclude the galaxies in which the main ionization mechanism is not driven by star formation (AGN-like galaxies). We chose the Ka03 curve. In order to consider a galaxy as a member of the main sequence, we therefore imposed a maximum [N II]/Hα of 0.48. We also discarded galaxies with very low emission in the diagram (LINER and passive galaxies). Finally, galaxies must be classified as blue with the color criterion and the ANN_C to be part of our sample. We found 1178 galaxies in total (SF sample hereafter).

[N II]/ Hα	Star-forming [%]	Seyfert [%]	Quiescent [%]
≤ 0.79 (S08)	89.8 ± 0.2	3.5 ± 0.2	6.7 ± 0.2
≤ 0.48 (Ka03)	72.8 ± 0.4	17.7 ± 0.4	9.4 ± 0.2
≤ 0.40 (Ke01)	62.4 ± 0.3	27.5 ± 0.4	10.1 ± 0.2

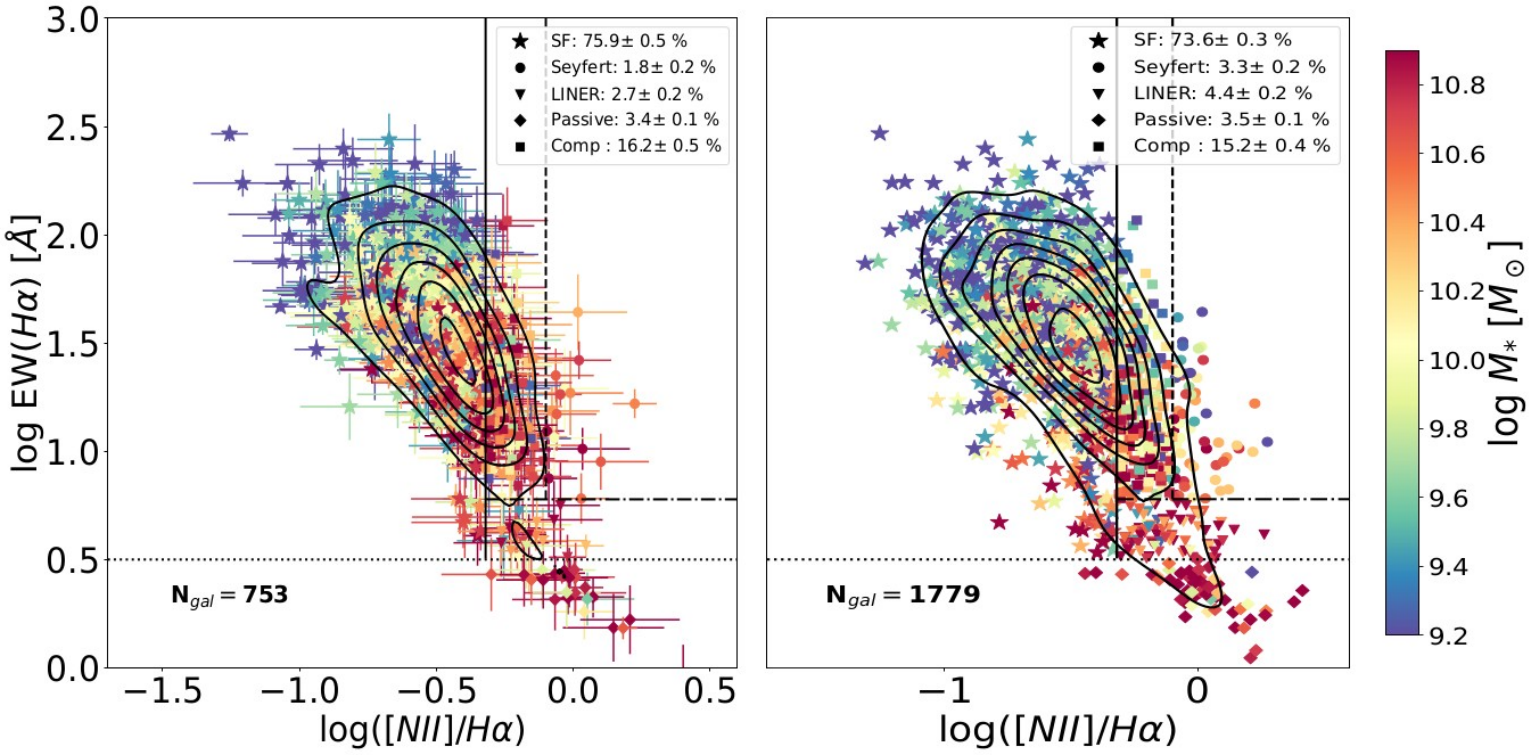

Fig. 8. WHAN diagram for galaxies with an error smaller than 0.2 dex (0.5 dex) in both the EW(Hα) and the [N II]/ Hα ratio in the left (right) panel. The errors are not shown in the right panel for clarity. The color bar indicates the stellar mass of the galaxy. The inset shows the relative percentage of each galaxy type in each subsample. Dashed and solid vertical lines define the optimal projections of the Ke01 and the Ka03 lines in the WHAN diagram (Cid Fernandes et al. 2010, 2011). Similarly, the dash-dotted horizontal line at EW(Hα) = 6 Å is the optimal transposition of the S07, and the dotted line at log EW(Hα) = 0.5 Å defines the limit of ELGs. In each panel, the galaxy counts are specified in the lower left corner. The parent sample contains 2154 galaxies. Density contours are drawn in black at the top.

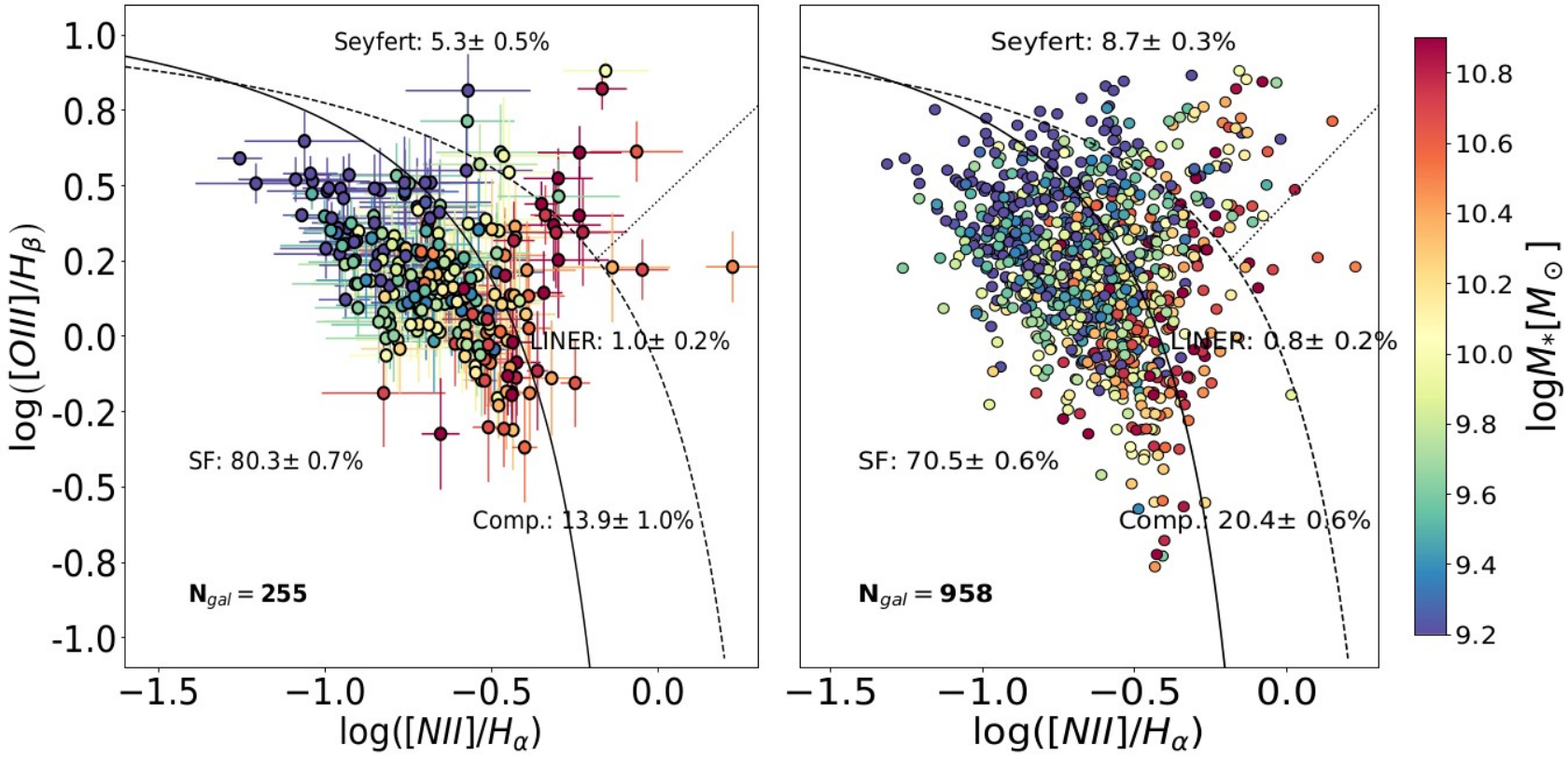

Fig. 7. BPT diagram for the galaxies in the sample with an error of 0.2 dex (0.5 dex) in the [O III]/Hβ and [N II]/Hα ratios in the left (right) panel. The errors are not plotted in the right panel for clarity. The color bar indicates the stellar mass of the galaxy. The solid (Ka03), dashed (Ke01), and dotted lines (S07) define the regions for the four main spectral classes. The relative percentage of each galaxy type in each subsample is indicated in the figure. In each panel, the number of galaxies is specified in the lower left corner. The parent sample contains 2154 galaxies.

The SFR was obtained from the Hα luminosity using the Kennicutt et al. (1994) relation converted to employ a Chabrier IMF (Chabrier 2003) and assuming case B recombination,

$$\mathrm{SFR}[M_\odot\ \mathrm{yr}^{-1}] = 4.9 \times 10^{-42} L_{\mathrm{H}\alpha}[\mathrm{erg/s}]. \quad (5)$$

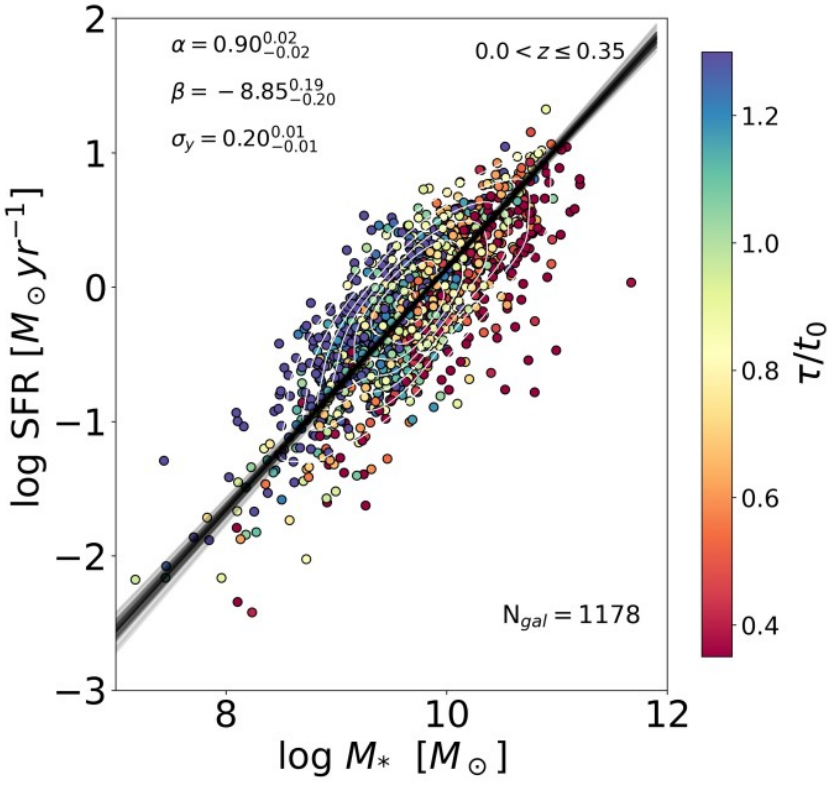

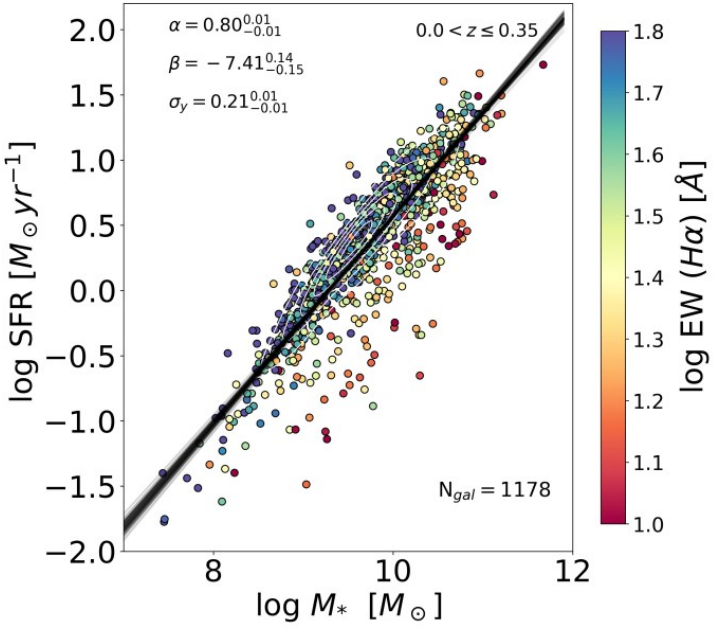

Fig. 15. SFR vs. stellar mass for the galaxy sample described in Sect. 5.1. SFRs are derived from `BaySeGal`. Galaxies are color-coded with the EW of Hα. Black lines are the best fits obtained with the Bayesian routine. The median posterior value and the 1σ confidence interval are shown for each of the parameters.

Differences between the SFR derived through Hα and the SED fitting

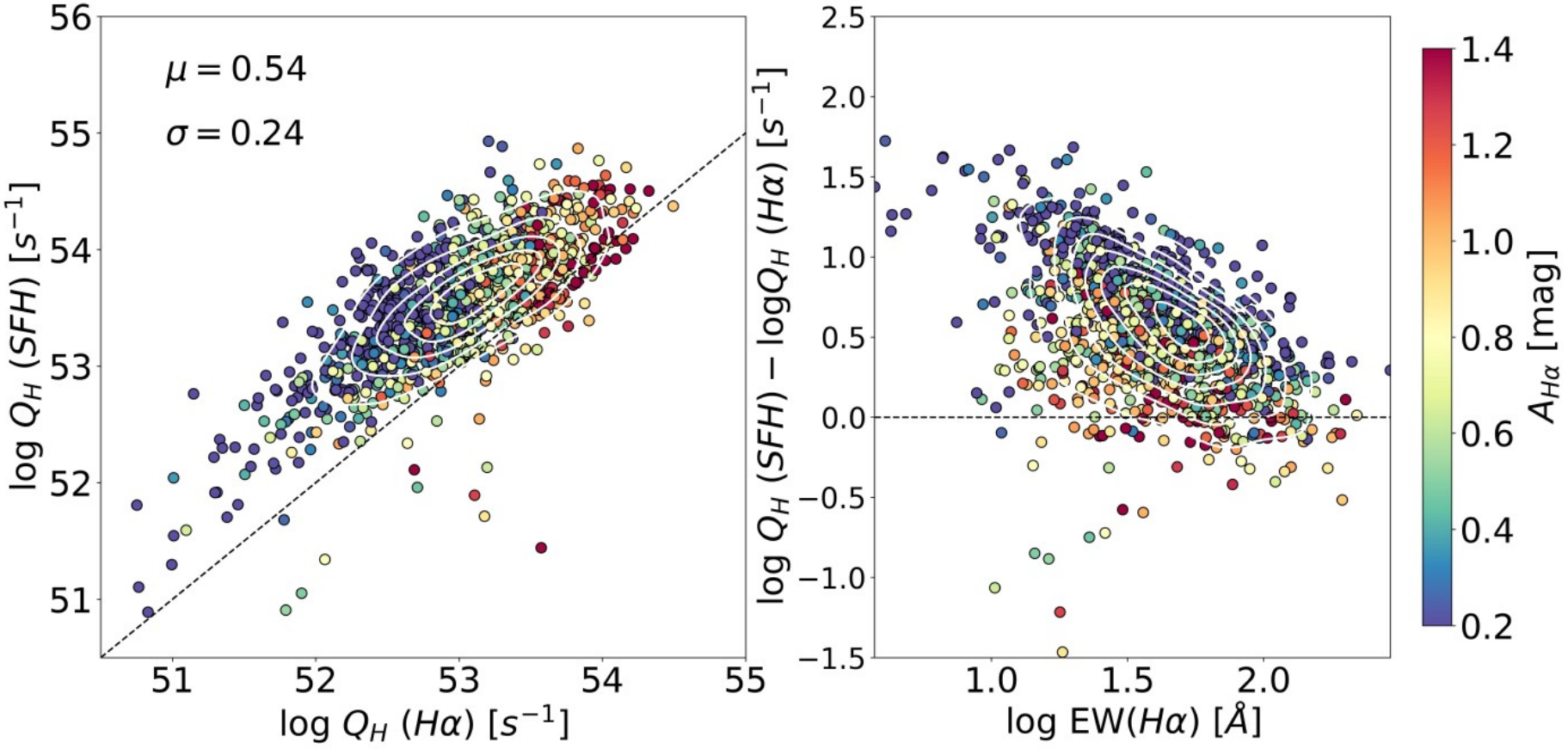

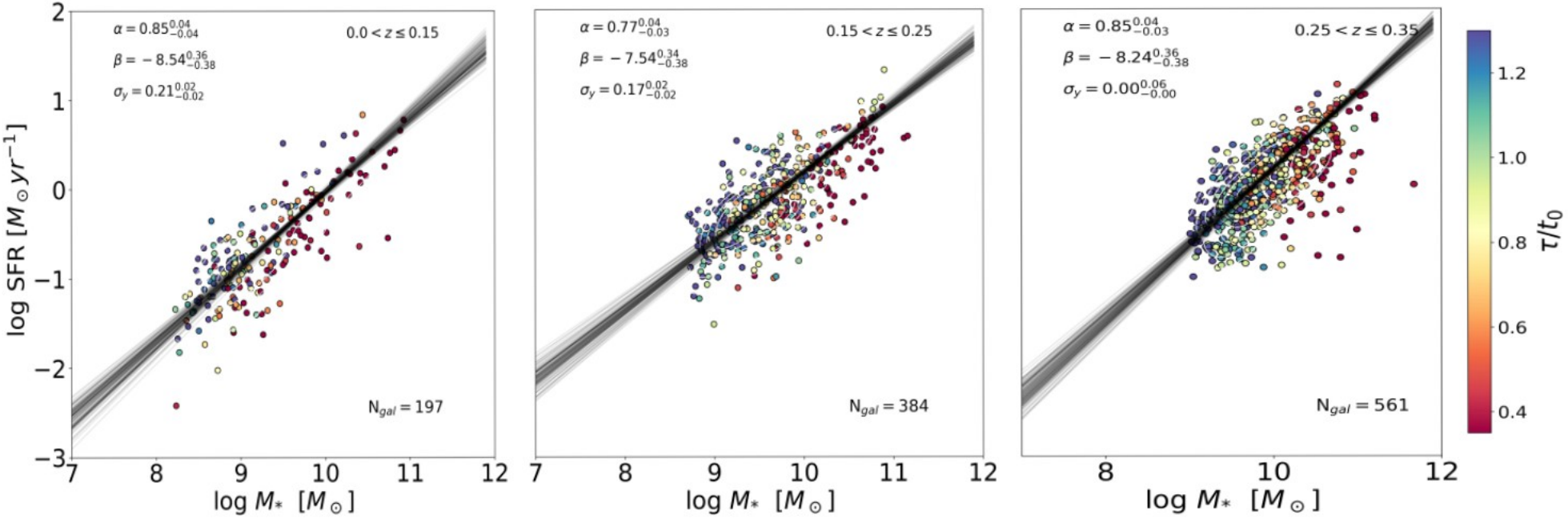

Fig. 13. SFR vs. stellar mass for galaxies in different redshift bins color-coded with their the τ/t_0 ratio (see Sect. 3.2.) Black lines are the best fits obtained with the Bayesian routine. The median posterior value and 1σ confidence interval are shown for each of the parameters. The number of galaxies within each redshift bin is also indicated.

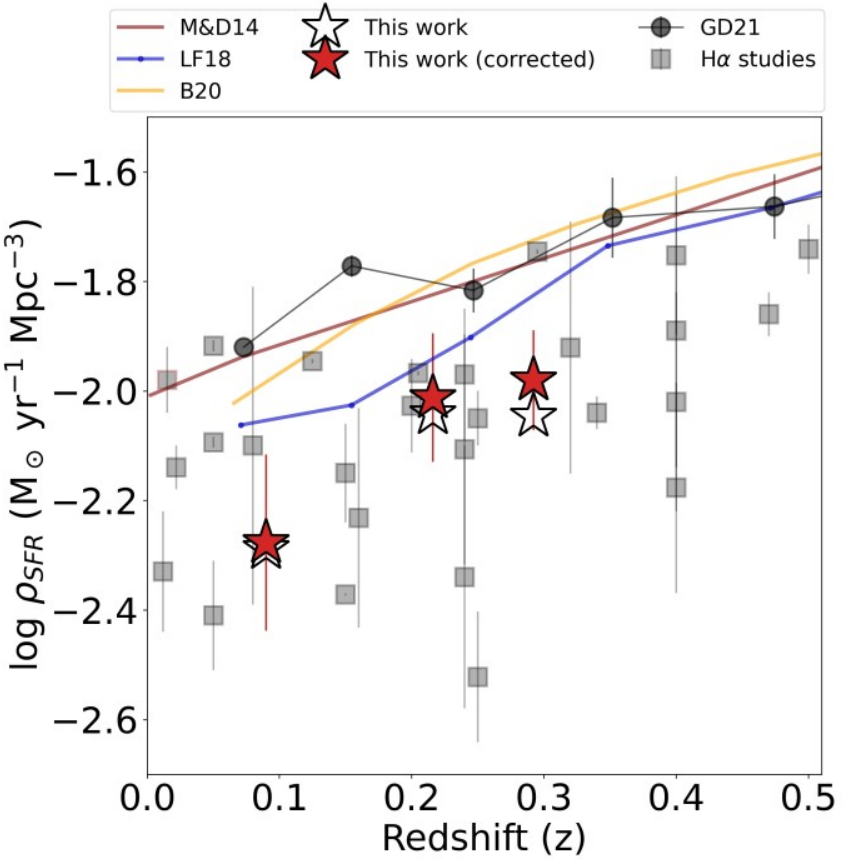

$$\rho^{int}_{\rm SFR} = \sum_{i \in j} \frac{\rm SFR_i}{V_{int}} w_i, \tag{12}$$

where $w_i = V_{int}/V_i^{max}$ is the weight that each galaxy has in the total $\rho^{int}_{\rm SFR}$, and V_{max} is the maximum volume occupied by a galaxy assuming that it cannot be observed at a magnitude fainter than 22.7. For galaxies with $V_{int} \leq V_i^{max}$, the weight is simply one, but galaxies with $V_{int} > V_i^{max}$ will contribute more.

Summary and conclusion

- 72.8 ± 0.4 %, 17.7 ± 0.4%, and 9.4 ± 0.2 % are SF, Seyfert, and passive or LINER galaxies, respectively.
- SFMS
- We tested the turnover-mass hypothesis by fitting a quadratic and a broken power law. However, we did not observe a flattening of the slope at high mass.
- Finally, we computed the cosmic evolution of the ρ SFR within three redshift bins: $0 < z \leq 0.15$, $0.15 < z \leq 0.25$, and $0.25 < z \leq 0.35$. We found agreement with previous measurements based on the Hα emission line. Nevertheless, we found an offset compared to the studies that derived ρ SFR from the SED fitting of the stellar continuum.